

热处理工艺对摩擦焊接钻杆力学性能的影响

朱 海¹, 郑海洋², 郭艳玲¹

(1. 东北林业大学 机电工程学院, 哈尔滨 150040;
2. 大庆钻井生产技术服务公司 钻井工具分公司, 黑龙江 大庆 163461)



朱 海

摘 要: 摩擦焊接钻杆要求其机械性能达到行业标准要求, 钻杆焊后的机械性能是由合理的焊接工艺和正确的热处理工艺保证的。通过对具体工艺生产的钻杆的检验结果进行分析, 探讨了如何根据焊后钻杆的力学性能和金相检测结果判断摩擦焊接钻杆不符合行业标准要求的原因, 分析了热处理工艺对钻杆力学性能的影响。结果表明, 当焊接工艺选择合理时, 焊缝的强度值低于标准, 冲击韧性值过高, 热处理热影响区硬度值偏低, 是由于淬火或回火工艺不合理造成的, 可通过调整淬火或回火工艺解决。

关键词: 摩擦焊; 石油钻杆; 热处理; 力学性能

中图分类号: TG113.25 文献标识码: A 文章编号: 0253-360X(2008)12-0093-04

0 序 言

石油钻杆是油田钻井设备上的重要零件。钻杆在使用过程中承受很大的拉应力和扭矩, 并经受强烈的震动和冲击^[1]。因此, 钻杆的力学性能必须满足一定要求。目前钻杆的生产和修复是采用摩擦焊工艺将钻杆接头和钻杆管体焊接而成。由于摩擦焊后焊缝得到的金相组织是混合组织, 造成焊缝区硬度分布不均匀, 局部区域硬度偏低, 而冲击韧性偏高, 满足不了使用要求, 因此, 焊后必须经过热处理调整焊缝区的金相组织和力学性能。通过采用合理的摩擦焊工艺和正确的焊后热处理工艺使摩擦焊接钻杆力学性能满足行业标准^[2]。钻杆生产中的力学性能应通过摩擦焊接过程和焊后热处理过程两方面保证。在钻杆批量生产前, 必须通过相应的检验, 确保采用的焊接和热处理工艺生产的钻杆满足标准要求。实际生产中发现, 钻杆生产厂家在生产钻杆时, 经过焊后检验, 发现力学性能达不到行业标准, 就首先判定焊接工艺不合理, 反复调整焊接参数。经过作者分析, 实际上多数是由焊后热处理工艺不正确造成的。

通过对比了两种热处理工艺对摩擦焊接钻杆力学性能的影响, 找出热处理工艺对力学性能的影响规律, 并对如何判断是焊接工艺还是热处理工艺不合理造成的力学性能不合格进行了探讨。为钻杆的

生产和修复提供一定指导。

1 试验方法

试验用钻杆规格为 5 英寸 G105, 焊接处外径 $\phi 130$ mm, 内径 $\phi 90$ mm。钻杆接头材料为 40CrMnMo, 管体为宝钢管体, 材质 35CrMo。摩擦焊机采用 MC-130, 焊机最大顶锻力 1 300 kN, 主电机功率 130 kW, 主轴转速 580 r/min, 顶锻焊接采用不刹车方式。采用的焊接工艺参数为: 一级摩擦压力 3 MPa, 二级摩擦压力 6.8 MPa, 三级顶锻压力 12 MPa。焊后热处理采用中频感应局部加热, 工艺流程是退火一去飞边一调质(淬火+高温回火)。中频电源频率 950 Hz, 退火和淬火加热功率 150 kW, 回火加热功率 90 kW。进行两组试验, 其中焊接工艺参数不变, 对比两种热处理工艺, 退火工艺不变, 改变淬火和回火工艺, 具体参数见表 1。

表 1 焊后热处理工艺参数
Table 1 Heat-treatment technology parameters

试验 编号	退火		淬火			回火	
	加热	保温	加热	保温	喷氮气	加热	保温
	温度 <i>T</i> /℃	时间 <i>t</i> /s	温度 <i>T</i> /℃	时间 <i>t</i> /s	时间 <i>t_p</i> /s	温度 <i>T</i> /℃	时间 <i>t</i> /s
1	900	300	890	180	180	680	480
2			910			640	360

准摩擦焊接钻杆焊区技术条件 SY/T5561 — 92”的要求进行拉伸、冲击、硬度、弯曲和金相等项目的检验。焊接接头拉伸和弯曲试验在 UH-I 型万能材料实验机上进行,焊接接头硬度在 HR-150D 型高行程电动洛氏硬度计上检验,冲击韧性在 JB-300WD 型冲击试验机上进行,金相分析采用 HAL100 金相显微镜。

2 试验结果

根据石油钻杆行业标准的要求进行了相应的检验,其中焊接接头力学性能检验结果见表 2,导向弯曲试验结果见表 3,焊接接头硬度检验结果见表 4,硬度检验位置见图 1,焊接接头硬度分布曲线及金相分析结果见表 5 和图 2~图 5。

表 2 焊区力学性能检验结果

Table 2 Mechanical properties of welding zone

试验 编号	试样 编号	屈服强度 R_{el}/MPa	抗拉强度 R_m/MPa	断后伸长率 $A(\%)$	冲击吸收功 A_{KV}/J
1	1—1	635	730	18.5	176
	1—2	599	685	20.0	154
	1—3	615	715	19.5	145
2	2—1	765	872	18.0	32
	2—2	755	890	18.0	46
	2—3	750	845	17.0	58
标准要求		≥ 655	≥ 724	≥ 13	最低值 ≥ 15 平均值 ≥ 20

表 3 导向弯曲试验结果

Table 3 Guided bend tests

试验 编号	试样		弯曲直径 D/mm	弯曲角度 $\theta/(\text{^\circ})$	试验结果	
	编号	取向			顺时针	逆时针
试验 1	1—1	纵向	40	150	未开裂	未开裂
	1—2	纵向	40	150	未开裂	未开裂
试验 2	2—1	纵向	40	150	未开裂	未开裂
	2—2	纵向	40	150	未开裂	未开裂

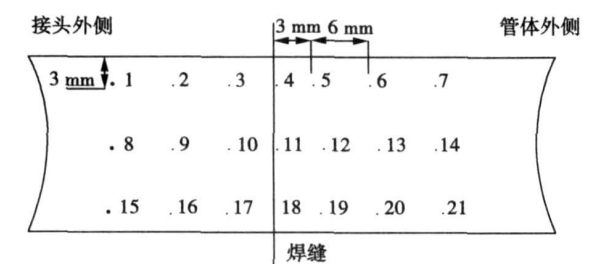


图 1 焊接接头硬度试验位置示意图
Fig 1 Hardness test profile

表 4 焊区硬度检验结果(HRC)

Table 4 Hardness of welding zone

试验位置	1	2	3	4	5	6	7
试验 1	29.0	29.5	28.5	25.5	22.7	21.9	21.0
试验 2	28.8	29.0	29.4	28.0	24.0	23.4	24.0
试验位置	8	9	10	11	12	13	14
试验 1	28.5	29.0	28.4	26.5	24.0	22.0	21.0
试验 2	30.0	30.0	29.5	29.0	25.0	24.0	24.0
试验位置	15	16	17	18	19	20	21
试验 1	30.0	29.1	28.7	26.4	22.0	21.4	21.6
试验 2	30.0	30.0	30.0	24.5	24.5	23.8	24.0

表 5 金相分析结果

Table 5 Metallographic analysis

检测位置	组织		晶粒度	
	试验 1	试验 2	试验 1	试验 2
管体	S 回	S 回	8.0 级	8.5 级
管体热影响区	S 回+F	S 回	9.5 级	9.5 级
焊缝管体侧	S 回+F	S 回	9.5 级	9.5 级
焊缝接头侧	S 回	S 回+	10 级	9.5 级
接头热影响区	S 回+F	S 回+少量 F	9.5 级	9.5 级
接头	S 回	S 回	8.5 级	8.5 级
标准要求	S 回	S 回	6 级	6 级

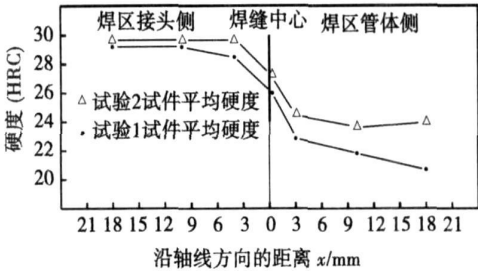


图 2 沿轴向方向焊接接头硬度分布
Fig 2 Hardness distribution along axis of specimen

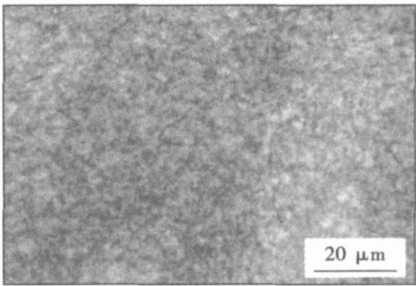


图 3 管体母材金相组织
Fig 3 Metallurgical structure of base metal

3 试验结果分析

从表 2 钻杆焊接接头力学性能检测结果得出,

在试验 1 的参数下,焊接的钻杆试件经检验冲击吸收功和断后伸长率均超过行业标准的要求,而屈服强度和抗拉强度值低于标准要求。由于摩擦焊接钻杆的力学性能是由摩擦焊接和焊后热处理两个工艺过程保证的,因此,首先要判定是哪个过程的工艺不合理造成的。从表 3 试件弯曲试验结果看,无论对试件进行顺时针还是逆时针弯曲,都达到弯曲角 150°不开裂,而且拉伸试验中试样断裂处位于距焊缝中心 20~22 mm 的管体侧,断裂位置已达管体母材热处理热影响区边界附近,而摩擦焊的焊接热影响区一般在 10 mm 左右,说明摩擦焊工艺已保证可靠的焊接。那么问题应该是出现在焊后热处理工艺上。根据金相分析结果,从表 5 和图 3 中看出接头和管体母材组织均为回火索氏体,晶粒度分别为 8.5 和 8.0 级。焊接后经局部中频感应调质处理,图 4 的金相图表明焊缝区及热处理热影响区的组织为回火索氏体+铁素体。显然,淬火加热得到的是奥氏体和铁素体,淬火加热不够充分,没有完全奥氏体化,淬火冷却后得到了马氏体+铁素体,经高温回火后分解为回火索氏体+铁素体。而且焊缝区及热处理热影响区的晶粒度为 9.5 级,比母材还要细小,说明淬火过程得到了细化的马氏体组织,因此淬火温度稍低,使调质后组织中有铁素体存在,势必使强度有所降低。从冲击韧性检验结果看,冲击功值已大

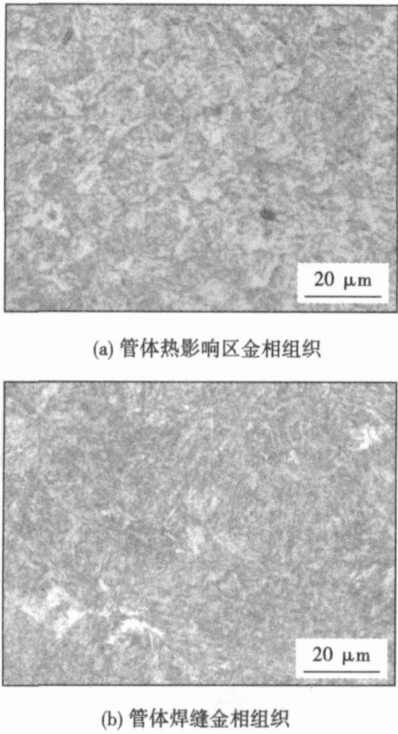


图 4 试验 1 试件金相组织

Fig. 4 Metallurgical structure of specimen 1

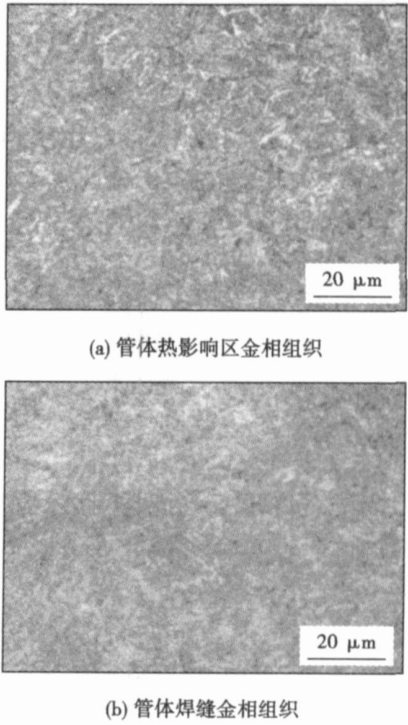


图 5 试验 2 试件金相组织

Fig 5 Metallurgical structure of specimen 2

大超过标准要求。

根据表 4 和图 2 分析焊区硬度检验结果,管体侧焊缝附近的硬度高,并沿母材方向逐渐降低,这是由于顶锻焊接时采用了不刹车形式,由于刹车减速度的减小,改善了接头金属的变形条件,使顶锻焊接过程中的应力状态发生有利变化,既有轴向镦粗,又有扭转,使塑性提高,形变量大大增加,形变区加宽。形变强化造成管体焊缝附近硬度和强度高于焊区管体其它部位^[3]。尽管硬度值都符合标准要求,但管体热处理热影响区内的硬度值偏低,热处理热影响区边界附近硬度值更低,平均值为 21.6 HRC。强度值也低于标准要求,拉伸断裂也发生在这个区域。钻杆的材料是属于 Cr-Mo 型合金调质钢,在进行调质处理时,随着回火温度的升高,强度、硬度下降,而韧性升高。因为试验钢的回火过程实质上就是过饱和的 α' 固溶体的脱溶过程,这个过程受 α' 相中 Cr, Mo 等合金元素的扩散控制,随回火温度升高, α' 基体的回复与再结晶的进行, C 原子的固溶强化效应不断下降,合金碳化物逐渐聚集并长大,对位错运动阻碍作用大大减弱,使屈服强度和抗拉强度不断下降^[4],又因硬度 (HB) 与抗拉强度近似为线形关系,故 HB 也降低。尽管当回火温度高于 500 °C 时,过饱和 C 原子已从 α' 固溶体中全部析出, C 原子的固溶强化作用消失。此时由于强碳化物形成元素 Mo 合金碳

化物的弥散析出, 钉扎位错运动, 起弥散强化的作用, 产生二次硬化效应, 抑制硬度和强度的降低。但是当回火温度高于 600 ℃时, 合金碳化物逐渐聚集并长大, 对位错运动阻碍作用大大减弱, 使硬度和强度急剧降低。同时, 随着回火温度的升高, 基体再结晶和碳化物质点粗化、球化, 由于碳化物的球化减少位错滑移的距离, 使滑移的距离变短, 位错不能切割它们, 故塑性、韧性呈上升趋势^[5]。因此, 从强度、硬度和冲击韧性检验结果综合分析, 造成强度低的原因主要是淬火温度低, 加热时没有完全得到奥氏体, 回火过程回火过强, 即回火温度偏高或回火时间过长。

为了调整摩擦焊接钻杆的力学性能达到行业标准要求, 在试验 2 方案中, 焊接工艺保持不变, 调整了淬火工艺和回火工艺, 将淬火温度由 890 ℃升高到 910 ℃, 将回火温度从 680 ℃降为 640 ℃, 保温时间从 480 s 降为 360 s。采用试验 2 的工艺焊接的钻杆试件经金相分析表明, 焊缝区和热处理热影响区组织为回火索氏体, 消除了铁素体组织 (见图 5); 晶粒度为 9.5 级, 可见淬火过程基本实现了奥氏体化, 且晶粒细小。从表 2 的力学性能检测结果看, 屈服强度和抗拉强度均已超过行业标准要求, 冲击韧性值降了下来, 但也远远超过行业标准要求。管体侧热影响区硬度有所提高, 热处理热影响区边界附近的平均硬度值上升到 23.8 HRC, 符合标准要求。弯曲试验结果表明, 无论对试件进行顺时针还是逆时针弯曲, 都达到弯曲角 150°不开裂。因此采用试验 2 的技术参数所焊接的钻杆各项性能指标均达到行业标准的

4 结 论

- (1) 摩擦焊接钻杆的力学性能是由合理的焊接工艺和正确的热处理工艺来保证的。
- (2) 摩擦焊接钻杆拉伸试验拉断在热处理热影响区, 弯曲试验没发生弯裂, 可证明焊接工艺是可靠的。
- (3) 摩擦焊接强度值低于标准, 冲击韧性值过高, 热处理热影响区硬度值偏低, 金相组织中有铁素体, 都是由于淬火温度低或回火过强造成的, 可通过提高淬火温度或降低回火温度、缩短保温时间解决。

参考文献:

[1] 朱张校, 王昆林, 贺茂文. 摩擦焊接钻杆焊缝断裂失效分析 [J]. 金属热处理, 1999(2): 36—38.

[2] 中国石油天然气总公司石油管材研究中心. SY/T 5561—92 摩擦焊接钻杆焊区技术条件 [S]. 北京: 中华人民共和国能源部, 1993.

[3] 朱海, 郭艳玲, 许明, 等. 刹车减速度对摩擦焊接头强韧性影响的研究 [J]. 热加工工艺, 2008(9): 75—77.

[4] 鲍静生. 淬火、回火温度对 35CrMoA 钢的力学性能及低温冲击的影响 [J]. 化工机械, 2001, 28(1): 16—18.

[5] 惠卫军, 董瀚, 翁宇庆, 等. 回火温度对 Cr-Mo-V 系高强度钢力学性能的影响 [J]. 金属学报, 2002, 38(10): 1009—1004.

作者简介: 朱海, 男, 1967 年出生, 博士研究生, 硕士生导师。主要从事材料成型工艺与过程控制, 金属材料强韧性方面的科研与教学工作。发表论文 10 余篇。

Email: zhuhai6060@163.com。

Finite element analysis of residual stress of welding repair for gas pipeline

YANG Linjuan^{1,2}, SHEN Shiming¹ (1. College of Mechanical and Power Engineering, Nanjing University of Technology, Nanjing 210009, China; 2. Science and Technology Administration Office, Nantong Vocational College, Nantong 226007, China). p77—80

Abstract By the finite element analysis software ABAQUS and the function of coupling process between heat and stress, the methods of entirety welding repair and local welding repair were simulated for 20-steel gas pipeline, and the distributions of the two kinds of welding residual stress were obtained. At the same time, the stress of welding-repair joint was analyzed by ABAQUS under inner pressure and welding residual stress. The results indicate that the residual stress of the entirety welding repair is lower than that of the local welding repair. And under inner pressure and welding residual stress, the tensile stress of the entirety welding repair is lower than that of the local welding repair too. It shows that the entirety welding repair joint is stronger than the local welding repair joint. The method of the entirety welding repair can reduce the probability of stress corrosion cracking and fit for the engineering application. The research results provide theory base for optimizing welding repair technology.

Key words: gas pipeline; entirety welding repair; local welding repair; welding residual stress; finite element analysis

Temperature control system of electron beam brazing joint

WANG Xuedong, LIU Peng, WANG Wei (Department of Mechanical Engineering, Tsinghua University, Beijing 100084, China). p81—84

Abstract: High precision digital PID control system used in temperature control of electron beam brazing joint was realized. In order to keep the predefined joint temperature during brazing process, digital control model and controller were constructed based on computer control and discrete control theories. The type of the controlled object was determined by open-loop and closed-loop step responses, and the effect of the expanded ultimate-sensitivity method and the expanded step-response method were compared when the PID parameters were tuning. The PID parameters obtained by the ultimate-sensitivity method were optimized by the through normalization on line, and each group of parameters and the corresponding experimental results were provided. Integration separation algorithm was also used to enhance the dynamic performances. The experimental results show that overshoot is so small that can be ignored and time is not needed to adjust; the temperature control precision can reach $\pm 2.5\text{ }^{\circ}\text{C}$.

Key words: electron beam brazing; closed-loop control; discrete control system

Effects of trace indium on properties and microstructure of Ag-Cu-Zn filler metal

LU Fangyan¹, XUE Songbai¹, ZHANG Liang¹, LAI Zhongnin^{1,2}, GU Liyong³, GU Wenhua³ (1. Nanjing University of Aeronautics and Astronautics, Nanjing 210016, China; 2. Jiangsu University of Science and Technology, Zhenjiang 212003,

China; 3. Changshu Huayin Filler Metals Co. Ltd., Changshu 215513, China). p85—88

Abstract Melting temperature, spreadability, microstructures of silver filler metal bearing different content of indium, and the mechanical properties of brazed joints were studied respectively. By using copper and brass plates as base metal, brazing with flame method, the mechanical properties of the joints brazed with lap-joint and butt joint were tested and analyzed at the same time. Results show that adding indium can decrease the melting temperature and improve the spreadability of the silver filler metal, and the microstructures of the silver filler metal bearing different content of indium are refined significantly. For the lap-joint of brass, the tensile strength of the joints gradually strengthens, presenting parabolic shape, with the increasing of the element indium; the fractures position of two kinds of brazed joints happens on the base metal, except for the lap-joint of brass, which shows better mechanical properties of the joints brazed with the silver filler metals bearing indium.

Key words: silver filler metal; melting temperature; spreadability; mechanical properties; microstructure

Microstructure and interface analysis of aluminum coating sprayed by electro-arc spraying on AZ91D magnesium alloy

MA Kai^{1,2}, SUN Daqian¹, XUAN Zhaozhi¹, LU Jia¹ (1. School of Materials Science and Engineering, Jilin University, Changchun 130022, China; 2. School of Mechanical and Electrical Engineering, Changchun Institute of Technology, Changchun 130012, China). p89—92

Abstract In order to obtain the excellent composite coating on magnesium alloy, double aluminum wires as two electrodes were automatically fed to create electric arc, the melting aluminum drops were sprayed on the AZ91D magnesium alloy surface by compressed air, and then the Mg-Al composite coating was formed. The optimum processing parameters were found by selecting different voltages and air pressure to carry on the spray experiments and analyzing the influence of the parameters on the coating structure performance. The characteristics of the coating microstructure and interface were researched by using the modern analysis methods, and the coating corrosion resistance was analyzed by test the coating electrode potential and the salt-spray experiment. The results indicate that certain voltage and air pressure can cause the coating to be compact. There is the newborn microstructure in the interface. The dual-structures of nano-scale crystal beam and micron-scale lamellar under 50 nm appear in the coating. The corrosion resistance of the coating surpasses that of the magnesium alloy matrix obviously.

Key words: magnesium alloy; arc spray aluminium; nano-crystalline; corrosion resistance

Effects of heat treatment technology on mechanical properties of friction welding drill rod

ZHU Hai¹, ZHENG Haiyang², GUO Yanling¹ (1. Mechanical and Electrical Engineering College, Northeast Forest University, Harbin 150040, China; 2. Drilling Tool Sub-company of Daqing Drilling Technology Services Company, Daqing 163461, China). p93—96

Abstract Mechanical properties of the friction weld drill rod, which is guaranteed with the rational welding technology and the rational heat treatment technology, must meet the requirements of profession standards. It is studied how to judge the cause of products being not up to standard. The effect of heat treatment technology on mechanical properties of the welded drill rods is analyzed. The results show that during the normal welding technology the yield intensity lower than that of profession standards, the impact ductility much higher than normal and the lower hardness in the heat treatment area are due to incorrect quench or temper technology. It can be corrected by revising quench or temper technology.

Key words: friction welding; drill rod; heat treatment; mechanical property

Taguchi method application for thermomechanical reliability in PBGA solder joint TAN Guangbin, YANG Ping, CHEN Zixia (School of Mechanical Engineering, Jiangsu University, Zhenjiang 212013, China). p97—100

Abstract: Taguchi method is applied to evaluate the solder joint reliability of PBGA (plastic ball grid array) under thermal cycling test by using nonlinear finite element method. The size and thickness of PCB (printed circuit board), the size and thickness of substrate, the diameter and height of solder joint, the thickness of die and the thickness of EMC are eight control factors that are selected to configure in L18 orthogonal array. The best control factor combination of PBGA can be decided as a combination with A₁, B₃, C₁, D₂, E₂, F₃, G₃, H₃ based on the optimization of Taguchi method, which solder joint diameter A, PCB size B, die thickness F and solder joint height G are four most important factors among them. The results show that the experimental data and predictive value of optimization are 2.87964 and 0.88286 larger than those of original state separately.

Key words: Taguchi method; plastic ball grid array; thermal cycling; solder joint

Method of hollow stud rotating arc welding WANG Kehong, ZHANG Deku, ZHENG Shixiong, GE Jiaqi (Research & Application Centre of Large Structural Work Welding Technology, Nanjing University of Science and Technology, Nanjing 210094, China). p101—103, 108

Abstract: Based on the idea of vertical divergent magnetic field making arc moving along the stud in wall, a new hollow stud rotating arc welding technology is presented. For hollow studs with outer-diameter of 12 mm and wall thickness of 3 mm, the homogeneous revolution of arc along stud wall is realized. Welding process experiments show that the process parameters of rotating arc stud welding are obviously greater than the same outer-diameter solid stud, and the welding technology normalized window is bigger, but narrower than that of solid stud. The optimum parameter of rotary arc current is 1—2 A, welding time is over 600—700 ms, welding current is 800—900 A. Joint performance testing results show that the formation of hollow stud welded joint is full and good. Macrostructure detection results show that there are no defect such as incomplete fu-

sion, slag and porosity, the interface fusion rate reaches 100%, and the interface strength maintains at 370—410 MPa.

Key words: rotating arc welding; hollow stud; stud welding

Friction welding technological parameter optimization based on LSSVM and AFSA SHU Fuhua (School of Mechanical and Electronic Engineering, Wuhan University of Technology, Wuhan 430074, China). p104—108

Abstract In order to determine friction welding technological parameters correctly and quickly, an optimization model for friction welding technological parameters based on least square support vector machine (LSSVM) and artificial fish-swarm algorithm (AFSA) was presented. With three friction welding technological parameters such as friction pressure, upset pressure and friction temperature as optimization parameters, welding joint tensile strength as optimization object, the nonlinear mapping relation between optimization parameters and optimization object was fitted by LSSVM. Firstly, experiments were taken to get data samples, and LSSVM model was established through data samples above. Then, the model was optimized by AFSA to get welding technological parameters. The results show that the construction model is easy, the optimization solution is quick, and the parameters optimized by this method make welding joint tensile strength increase by 2.1% comparing with that parameters optimized by orthogonal regression method.

Key words: friction welding; technological parameter; optimization; least square support vector machine; artificial fish-swarm algorithm

Three-wire MAG high speed welding process HUA Xueming¹, MA Xiaoli¹, LIN Hang¹, WANG Fei¹, WU Yixiong¹, Yasuhiko ONIKI², Shigen KAMIFUJI², SHI Jiangang² (1. Shanghai Key Laboratory of Materials Laser Processing and Modification, Shanghai Jiaotong University, Shanghai 200240, China; 2. Tsuneshi Holdings Corporation, Hiroshima 7200393, Japan). p109—112

Abstract A new technology of three-wire MAG high speed welding is researched to replace two-wire welding technology which is usually used to weld fillet in shipyard and the welding speed is under 1.0 m/min. Three wires, namely, leading wire, middle wire and trailing wire, are arranged in tandem. Each wire is equipped with separate wire feeder system, power supply and gas shield device, and welding process parameters can be adjusted individually to meet the various requirements of welding. The results show that the polarity combination of leading wire (DCEP)/middle wire (DCEN)/trailing wire (DCEP) or that of leading wire (DCEN)/middle wire (DCEP)/trailing wire (DCEN) can obtain stable welding process, good weld appearance, symmetrical weld seam, non-porous weld to meet the requirements of the shipbuilding industry; the maximum welding speed can be up to 1.8 m/min and the length of fillet weld leg can be to 5—8 mm by selecting a suitable welding current and welding speed. This new welding technology can be widely used for high-speed fillet welding industry.

Key words: three-wire welding technology; high-speed welding; GMAW; fillet welding